

## PAPER

# Effect of inserting a Helmholtz resonator on sound insulation in a double-leaf partition cavity

Satoshi Sugie<sup>1,\*</sup>, Junichi Yoshimura<sup>1</sup> and Teruo Iwase<sup>2</sup>

<sup>1</sup>*Kobayasi Institute of Physical Research,*

*Higashi-motomachi 3-20-41, Kokubunji, 185-0022 Japan*

<sup>2</sup>*Department of Architecture, Faculty of Engineering, Niigata University,*

*8050, Igarashi ni-no-cho, Nishi-ku, Niigata, 950-2181 Japan*

(Received 8 July 2008, Accepted for publication 28 January 2009)

**Abstract:** We investigated the improvement of sound insulation of a double-leaf partition using Helmholtz resonators. We proposed a method of predicting the sound reduction index  $R_0$  at normal incidence using impedance transfer, under the assumption that the resonators installed in the air cavity between the two leaves were independent components of a wall, similarly to boards and studs. Furthermore, for experimentation, a small sample without studs was used to prevent flanking transmission through them. Theoretical and empirical examinations revealed that installing the resonators in the cavity in the following manner was sufficient to control sound insulation at low frequencies. High sound insulation occurred at the resonance frequency  $f_0$  of resonators; the sound insulation decreased at higher and lower frequencies than  $f_0$ . The sound insulation at  $f_0$  depended on the acoustic resistance of resonators. When an air layer existed behind the resonators, other peaks and dips appeared at higher frequencies than  $f_0$ . Installing both a fibrous absorber and resonators in the cavity was sufficient to recover the decreased performance of sound insulation owing to the installation of resonators.

**Keywords:** Helmholtz resonator, Double-leaf partition, Sound reduction index, Acoustic impedance, Small sample

**PACS number:** 43.55.Rg [doi:10.1250/ast.30.317]

## 1. INTRODUCTION

A double-wall structure improves the sound insulation compared with a single wall. However, it has not only advantages, but also disadvantages for sound insulation. The most important advantage of the double-leaf partition is that it provides higher performance in sound insulation than a single partition of the same weight. However, sound insulation is decreased by such disadvantages as sound bridges through studs and frames, overlap of the coincidence effect, and mass-air-mass resonance.

Several studies have been undertaken to mitigate these disadvantages. To control the sound bridges, the two leaves must be mounted on studs that are mutually independent. Then the leaves must be connected resiliently to the studs. To avoid the overlapping of coincident frequencies, it is common to use leaves of different thickness.

However, it is difficult to improve sound insulation at low frequencies in the range that includes the mass-air-

mass resonance frequency  $f_{\text{rmd}}$ . To shift  $f_{\text{rmd}}$  to a lower frequency and to improve the sound insulation, the weight of boards and the thickness of the air layer are increased. However, this is not the best strategy because it increases the wall's total weight and thickness. Installing fibrous absorbers in the cavity improves sound insulation only at mid- and high frequencies; these absorbers have less effect on sound insulation at low frequencies including  $f_{\text{rmd}}$  [1–4].

To recover the loss of sound insulation at low frequencies, several investigations have been undertaken using Helmholtz resonators, which have high absorption for a narrow frequency range despite their small volume, in the cavity of a double-leaf partition. For example, Narang [5] modified conventional steel studs to form slit resonator studs and investigated the potential of improving sound insulation of the wall using slit resonator studs through an empirical approach. Their resonance frequency was tuned to be higher than  $f_{\text{rmd}}$  of the wall. Therefore, the improvement of sound insulation through the use of slit resonator studs remained slight: only 1–2 dB in sound insulation.

\*e-mail: sugie@kobayasi-riken.or.jp

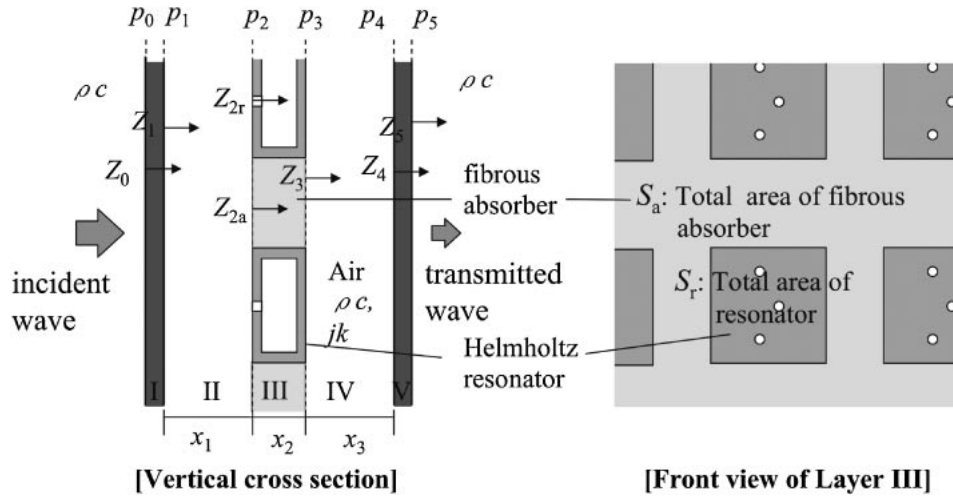


Fig. 1 Theoretical model of double-leaf partition with Helmholtz resonators.

Prydz *et al.* [6] provided two prediction methods of sound insulation of a wall having many resonators combined uniformly with the whole surface of a board; Mason and Fahy [7] presented a prediction of sound insulation for a wall with resonators set in the frame of the cavity, such as a double window. They showed that the sound insulation decreased upon the insertion of resonators at higher and lower frequencies than the resonance frequency  $f_0$  of resonators, although it increased drastically at  $f_0$ . However, they did not suggest any means of improvement for those frequencies at which sound insulation decreased. Therefore, if the sound insulation were improved at those frequencies, although the advantage of the resonator would remain, installing resonators in the cavity would also become useful for improving the sound insulation at low frequencies.

The resonators, however, were fixed on components of the wall, such as boards and frames, in the above-named investigations. Thus, if resonators could be set anywhere in the wall, the sound insulation could be changed freely, and it might be increased in a wide range of low frequencies. Therefore, the disadvantages of resonators in terms of sound insulation would be ameliorated. As described in this paper, we investigated the effect of resonators placed independently of the wall components, because the above researchers did not study the effect of resonators under this condition and the sound insulation could not be calculated by their methods. Concretely speaking, we derived a method of predicting sound insulation at normal incidence for the double-leaf partition with Helmholtz resonators installed in the cavity, when resonators were assumed to be placed arbitrarily in the cavity.

According to not only the theoretical prediction but also the experiment, we considered the dependence of the sound insulation of the double-leaf partition on the absorption performance and position of installed resona-

tors. We discussed the effectiveness of the combination of resonators and fibrous absorbers in improving the sound insulation in a wide range of low frequency. In these cases, the resonance frequency  $f_0$  of resonators was tuned to  $f_{\text{rmd}}$  of the wall to change the sound insulation drastically in the region around the mass-air-mass resonance frequency  $f_{\text{rmd}}$  of the wall.

## 2. PREDICTION OF SOUND INSULATION

### 2.1. Sound Reduction Index of Double-Leaf Partition

The sound reduction index  $R_0$  at normal incidence is calculable by the impedance transfer method [8,9]. In the acoustical model, the double-leaf partition is assumed to be a multilayer structure, as shown in Fig. 1. Layers I and V are board layers, Layers II and IV are fibrous absorber layers or air layers, and Layer III is combination of Helmholtz resonators and of the fibrous absorber or air. Figure 1 shows that they are arranged periodically. The feature of this prediction method is that two different materials can be treated in a single layer. Sound waves approach the surface of the left-hand side of the wall and permeate into it at normal incidence against the wall. Ultimately, sound waves are transmitted through each layer and radiate from the right-hand side. The sound transmission coefficient  $\tau$  and the reduction index  $R_0$  of the wall at normal incidence can be expressed as

$$\frac{1}{\tau} = \left| \frac{Z_0 + \rho c}{2Z_0} \right| \left| \frac{p_0}{p_1} \frac{p_1}{p_2} \frac{p_2}{p_3} \frac{p_3}{p_4} \frac{p_4}{p_5} \right|^2, \text{ and} \quad (1)$$

$$R_0 = 10 \log \left( \frac{1}{\tau} \right), \quad (2)$$

where  $p_i/p_{i+1}$  is the ratio of sound pressure on both sides of the  $i+1$ -th layer,  $Z_0$  is the acoustic impedance of the surface of Layer I (board) at normal incidence,  $\rho$  is the air density, and  $c$  is the sound velocity in air.

## 2.2. Sound Pressure Ratio and Acoustic Impedance on Layers I and V

The target frequencies are low frequencies including the mass-air-mass resonance frequency  $f_{\text{rmd}}$ . Therefore, these layers can be treated as an infinite plate (surface density  $m_{i+1}$ ) vibrating in a body. Then, the acoustic impedance  $Z_i$  at the left-hand side of these layers is obtainable as

$$Z_i = j\omega m_{i+1} + Z_{i+1}, \quad (3)$$

where  $i = 0$  and/or 4,  $Z_{i+1}$  is the acoustic impedance at the left-hand-side of the next layer,  $\omega$  is the angular frequency equivalent to  $2\pi f$ , and  $f$  is the frequency. Because the values of the particle velocity on both sides of the board layer are equal, the ratio  $p_i/p_{i+1}$  of sound pressure on the two sides of this layer is calculable as

$$\frac{p_i}{p_{i+1}} = 1 + \frac{j\omega m_{i+1}}{Z_{i+1}}, \quad (4)$$

where  $Z_{i+1}$  of Layer V is equal to  $\rho c$ , which is the characteristic impedance of air.

## 2.3. Sound Pressure Ratio and Acoustic Impedance on Layers II and IV

Representing the propagation constant and the characteristic impedance of an absorber or air as  $\gamma_{i+1}$  and  $Z_{c,i+1}$ , respectively, the acoustic impedance  $Z_i$  on the left-side surface of this layer and the ratio  $p_i/p_{i+1}$  of sound pressure on both sides of this layer are calculated, respectively, as

$$Z_i = Z_{c,i+1} \frac{Z_{i+1} \cosh(\gamma_{i+1}x_i) + Z_{c,i+1} \sinh(\gamma_{i+1}x_i)}{Z_{i+1} \sinh(\gamma_{i+1}x_i) + Z_{c,i+1} \cosh(\gamma_{i+1}x_i)}, \text{ and } (5a)$$

$$\frac{p_i}{p_{i+1}} = \cosh(\gamma_{i+1}x_i) + \sinh(\gamma_{i+1}x_i) \frac{Z_{c,i+1}}{Z_{i+1}}, \quad (5b)$$

where  $i = 1$  and/or 3,  $x_i$  is the  $i + 1$ -th layer thickness, and  $Z_{i+1}$  is the acoustic impedance at the left-side surface of the next layer. When the medium of the layer is air,  $\gamma_{i+1}$  and  $Z_{c,i+1}$  can be written as

$$\gamma_{i+1} = jk \text{ and } (6a)$$

$$Z_{c,i+1} = \rho c, \quad (6b)$$

where  $k$  is the wave number in air. When the layer medium is a fibrous absorber, it can be described using the following empirical relationships [10].

$$Z_{c,i+1} = \rho c \left\{ 1 + 0.070 \left( \frac{f}{\sigma} \right)^{-0.632} - j0.107 \left( \frac{f}{\sigma} \right)^{-0.632} \right\} \quad (7a)$$

$$\gamma_{i+1} = \frac{\omega}{c} \left[ \left\{ 0.160 \left( \frac{f}{\sigma} \right)^{-0.618} \right\} + j \left\{ 1 + 0.109 \left( \frac{f}{\sigma} \right)^{-0.618} \right\} \right] \quad (7b)$$

Therein,  $\sigma$  is the airflow resistivity of the fibrous medium.

## 2.4. Sound Pressure Ratio and Acoustic Impedance on Layer III

The arrangement of Helmholtz resonators and of the fibrous absorber or air is presented in Fig. 1. In this layer, they are set parallel to the sound wavefront and are arranged periodically at regular intervals. In this calculation, this layer is divided into the fibrous absorber area and the resonator area, and the acoustic impedance and the ratio of sound pressure are derived for them.

In the fibrous absorber, if sound pressure  $p_2$  on the surface of the left-hand side of this area is uniform, the acoustic impedance  $Z_{2a}$  on the left-side surface of this area and the ratio  $p_2/p_{3a}$  of sound pressures on the two sides of this area are calculable respectively according to Eqs. (5a) and (5b), as

$$Z_{2a} = Z_{c,3a} \frac{Z_3 \cosh(\gamma_3 x_2) + Z_{c,3a} \sinh(\gamma_3 x_2)}{Z_3 \sinh(\gamma_3 x_2) + Z_{c,3a} \cosh(\gamma_3 x_2)} \text{ and } (8a)$$

$$\frac{p_2}{p_{3a}} = \cosh(\gamma_3 x_2) + \sinh(\gamma_3 x_2) \frac{Z_{c,3a}}{Z_3}, \quad (8b)$$

respectively where  $p_{3a}$  is the sound pressure at the right-side surface of the fibrous area and  $Z_3$  is the acoustic impedance at the left-side surface of Layer IV.

In the resonator area, assuming that the acoustic impedance  $Z_{2r}$  on the surface of the resonator area is treated as a concentrated constant, the ratio  $p_2/p_{3r}$  of sound pressures on the two sides of this area is equal to the ratio of acoustic impedances on the two sides, similarly as derived for Eq. (4). Therefore, the ratio  $p_2/p_{3r}$  of sound pressures on the two sides of this area is calculated as

$$\frac{p_2}{p_{3r}} = \frac{Z_{2r} + Z_3}{Z_3}, \quad (9)$$

where  $p_{3r}$  is the sound pressure at the right-side surface of the resonator area.

In fact,  $p_3$  corresponds to the average of  $p_{3a}$  and  $p_{3r}$ , as below, if sound pressure  $p_3$  on the surface of the right-hand side of this area is also uniform:

$$p_3 = \frac{1}{S_a + S_r} (S_a p_{3a} + S_r p_{3r}), \quad (10)$$

where  $S_a$  is the total area of the fibrous absorber area and  $S_r$  is the resonator area, as presented in Fig. 1. The share  $\phi$  of the resonator's occupation in this layer is defined as

$$\phi = \frac{S_r}{S_a + S_r}. \quad (11)$$

Combining Eqs. (10) and (11) gives the average ratio  $p_2/p_3$  of sound pressures on the two sides of this layer as

$$\frac{p_2}{p_3} = \left( \frac{p_{3r}}{p_2} \phi + \frac{p_{3a}}{p_2} (1 - \phi) \right)^{-1}. \quad (12)$$

Because the fibrous absorber area and the resonator area are arranged in parallel in this layer to the wave surface, the average acoustic impedance  $Z_2$  on the left-hand side of this layer can be expressed as

$$Z_2 = \left( \frac{\phi}{Z_{2r}} + \frac{1-\phi}{Z_{2a}} \right)^{-1}. \quad (13)$$

The acoustic impedance on resonators is derived next. Defining that the number of holes on the resonator is  $n$  and the diameter is  $d$ , the open area ratio  $\psi$  of holes is defined as

$$\psi = \frac{n(d/2)^2\pi}{S}, \quad (14)$$

where  $S$  is the area of the front surface in a resonator. The acoustic impedance  $Z_{2r}$  on the surface of the Helmholtz resonator is calculable as

$$Z_{2r} = \frac{1}{\psi} \left[ R_h + j \left\{ \omega \rho (t + 0.85d) - \frac{(d/2)^2 \pi n \rho c^2}{\omega V} \right\} \right], \quad (15)$$

where  $V$  is the resonator's air gap volume and  $t$  is the hole depth. The acoustic resistance  $R_h$  is obtainable as [11]

$$R_h = \frac{4\pi(d/2)t(\pi\rho\eta f)^{1/2}}{\pi(d/2)^2}, \quad (16)$$

where  $\eta$  represents the viscosity of air. This value is  $1.8 \times 10^{-5}$  kg/m s.

### 3. VERIFYING PREDICTED VALUES BY EXPERIMENTS

#### 3.1. Measuring Method and Specimen

The level difference  $D$  between the two sides of the specimen was measured as the frequency characteristics of sound insulation, and the intensity sound reduction index  $R_1$ , according to ISO 15186-1 [12], was also measured to verify typical values of sound transmission loss. Test rooms for the conventional two-room method, in compliance with ISO 140-3 [13], were used. Many absorbers were placed in the receiving room to satisfy ISO 15186-1 requirements. Multiple sound sources were used; three omnidirectional loudspeakers were driven at the same level by mutually uncorrelated signals. The filler wall, which had sufficiently higher sound insulation than the specimen, was built into the test opening between test rooms. The specimen was placed in the wall, as presented in Fig. 2. A microphone was set on either side of the specimen for level difference  $D$  measurements [14], as presented in Fig. 2. The microphones were at the center of the specimen. They almost touched the surface of the specimen (about 10 mm distance).

Figure 3 shows that the double-leaf partition specimen comprises two 5-mm-thick acrylic boards and the cavity, where the distance of separation is 112 mm. The mass-air-

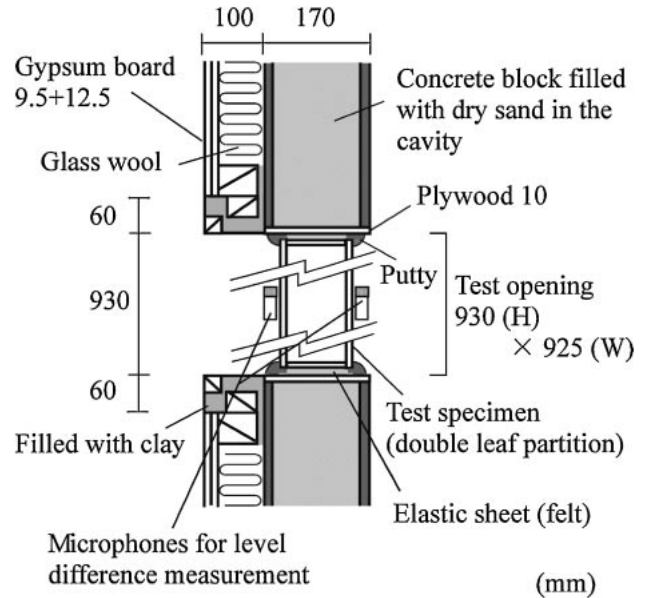


Fig. 2 Vertical cross section of the specimen and filler wall.

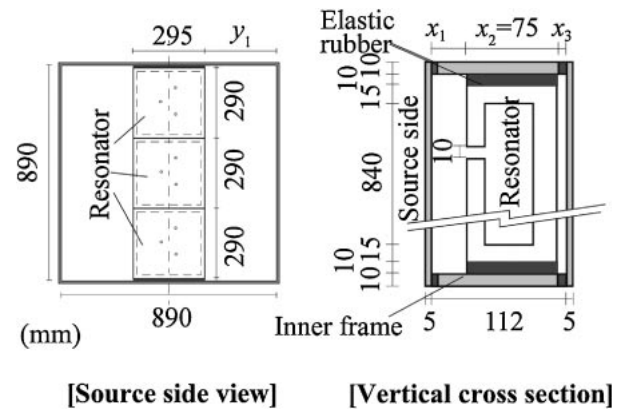


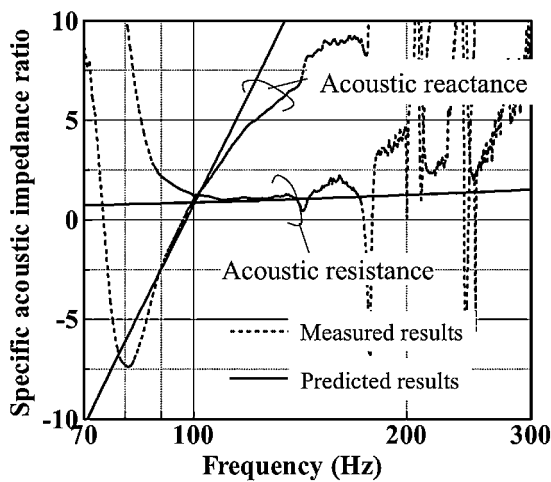
Fig. 3 Structure of specimen.

mass resonance frequency  $f_{\text{rmd}}$  of this double-leaf partition was calculated as 103 Hz. Both boards were 0.89 m  $\times$  0.89 m; no studs were present in the cavity. The boards had no direct contact with the inner frame because we used rubber cushioning; the boards were merely pressed to the inner frame using putty, thereby reducing the vibration transmission through the inner frame.

Each resonator installed in the wall cavity was made of a 15-mm-thick acrylic board with three 10-mm-diameter and 15-mm-deep holes. The resonator's air gap volume was 265  $\times$  260  $\times$  45 mm. Its theoretical resonance frequency  $f_0$  was calculated to be 98 Hz, which was almost equal to  $f_{\text{rmd}}$  of the wall. Figure 3 shows that three resonators were arranged vertically in the air cavity. The position  $(x_1, y_1)$  is (37 mm, 298 mm). Therefore, the share  $\phi$  of the resonators' s occupation in layer III was 0.33 and the open area ratio  $\psi$  of holes in the resonator was 0.0028. Table 1 shows other details of the specimen.

**Table 1** Properties of double-leaf partition and resonators.

Double partition:		
Acrylic board thickness	—	5 mm
Air layer's thickness	$x_1 + x_2 + x_3$	112 mm
Mass-air-mass resonance frequency	$f_{\text{rmd}}$	103 Hz
Resonators:		
Thickness of a resonator	$x_2$	75 mm
Air gap volume of a resonator	$V$	$3.1 \times 10^{-2} \text{ m}^3$
Surface area in a resonator	$S$	$8.6 \times 10^{-2} \text{ m}^2$
Number of resonators	—	3
Share of resonators' occupation	$\phi$	0.33
Depth of hole	$t$	15 mm
Diameter of hole	$d$	10 mm
Number of holes	$n$	3
Open area ratio of holes in a resonator	$\psi$	$2.8 \times 10^{-3}$
Resonance frequency	$f_0$	98 Hz
Position of resonator	$x_1, y_1$	37 mm, 298 mm

**Fig. 4** Measured and predicted results of acoustic impedance of resonator at normal incidence.

### 3.2. Comparisons between Predicted and Measured Results

The acoustic impedance of the resonator at normal incidence was measured using the impedance tube, which had a  $300 \times 300$  mm inner size. Figure 4 presents the measured results and those calculated using Eqs. (15) and (16). The results are shown as ratios to the characteristic impedance of air. A decrease in the sound pressure in the dips of standing waves occurred in the impedance tube, resulting in many peaks and dips of acoustic impedance in the measured results. Around the resonance frequency  $f_0$ , where the imaginary part of the acoustic impedance is equal to zero, the calculated results coincide approximately with measured ones, but they are not in agreement with the measured ones at the other frequencies. However, the

frequency range around  $f_0$  is important for estimating the sound insulation because the sound insulation of a wall having resonators will be increased considerably at  $f_0$ . Therefore, Eqs. (15) and (16) are suitable for calculating the sound insulation when  $f_0$  is tuned to  $f_{\text{rmd}}$  of the wall.

Next, Figs. 5 and 6 respectively depict the measured and the predicted results of sound insulation of the double-leaf partitions with and without the resonators in the cavity of the wall. Figure 5(a) and 5(b) respectively depict level difference  $D$  and the intensity sound reduction index  $R_1$ . Figure 6(b) also shows results calculated on the one-third octave band from results in Fig. 6(a) for comparison with Fig. 5(b).

The measured and predicted results cannot be compared quantitatively, because the sound wave is normally incident in the prediction, while it is incident at random in measurement. However, it is possible to compare the frequency characteristics under the two conditions, because it has been established experimentally that the frequency characteristics of the sound insulation at normal incidence is not so different from that at oblique incidence at low frequencies, from a literature review [15].

The components of the double-leaf partition have infinite size in the prediction, but they have finite size in the measurement. Therefore, some peaks and dips appear in the measured results in Figs. 5(a) and 5(b) because resonances other than mass-air-mass resonance occur on the boards and in the air cavity. However, those peaks and dips cannot be predicted by our method. Figure 5(a) shows that the measured results for the specimen without a resonator in the cavity decrease sharply at the mass-air-mass resonance  $f_{\text{rmd}}$ . On the other hand, upon installing resonators in the cavity,  $D$  increases at  $f_0$ , but, decreases on both sides of  $f_0$ . Figure 5(b) shows that  $R_1$  also rises sharply at the 100 Hz band, which includes the resonance frequency  $f_0$  of the resonator, but decreases at 125 Hz band. Therefore, although only a microphone is set on either side of the specimen in the measurement of level difference,  $D$  and  $R_1$  show similar tendencies.

Predicted results in Figs. 6(a) and 6(b) show that installing resonators in the cavity increases the sound insulation of the double-leaf partition at  $f_0$  and decreases it on both sides of  $f_0$ , similarly to measured results. This tendency also corresponds to those described in past reports [6,7]. A comparison of Figs. 5 and 6 show that the difference between the values of sound insulation with and without resonators in the calculated results almost agrees with the difference in the measured results. This prediction can qualitatively explain the effect of inserting a Helmholtz resonator in a cavity on sound insulation of a double-leaf partition.

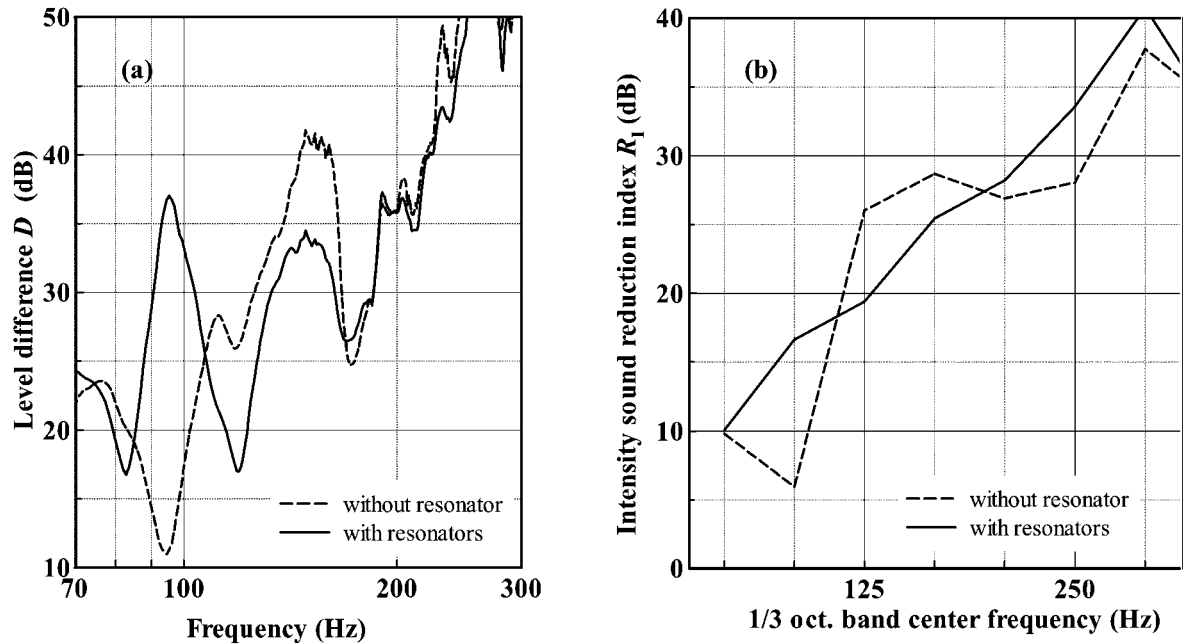


Fig. 5 Measured sound insulation with and without resonator (position  $x_1 = 37$  mm) in the cavity of wall.

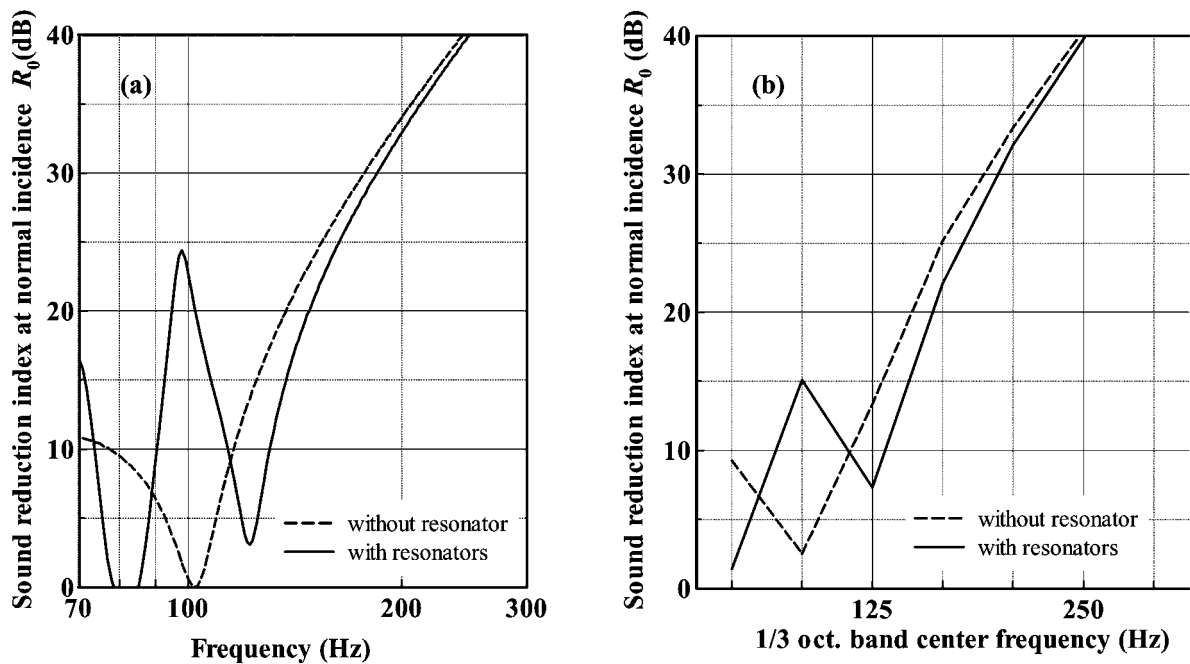


Fig. 6 Predicted sound insulation with and without resonator (position  $x_1 = 37$  mm) in the cavity of wall.

#### 4. EFFECT OF RESONATORS AND IMPROVEMENT OF SOUND INSULATION

##### 4.1. Relationship between Acoustic Impedance of Resonator and Sound Insulation

Although the resonance frequency of the resonator is maintained constant, its acoustic resistance on the surface can be changed by tuning the diameter and the number of opening holes of the resonator, according to Eq. (16). Figures 7 and 8 show calculated results of the acoustic

resistance of the resonator and sound insulation, respectively, for some various number  $n$  and diameter  $d$  of the hole when the resonance frequency  $f_0$  is kept at 98 Hz. Table 1 shows the properties of the resonator and the double-leaf partition, except  $d$  and  $n$ . The measured results of sound insulation are also shown in Fig. 9 under the same conditions as those of the calculation described above.

Figure 7 shows that the acoustic resistance decreases with decreasing number  $n$  and increasing diameter  $d$ . The sound insulation at  $f_0$  increases greatly with decreasing

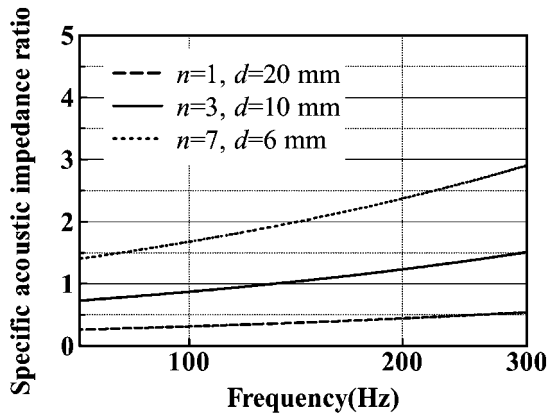


Fig. 7 Variation of acoustic resistance at normal incidence of resonator with number  $n$  and diameter  $d$  of holes, when  $f_0 = 98$  Hz.

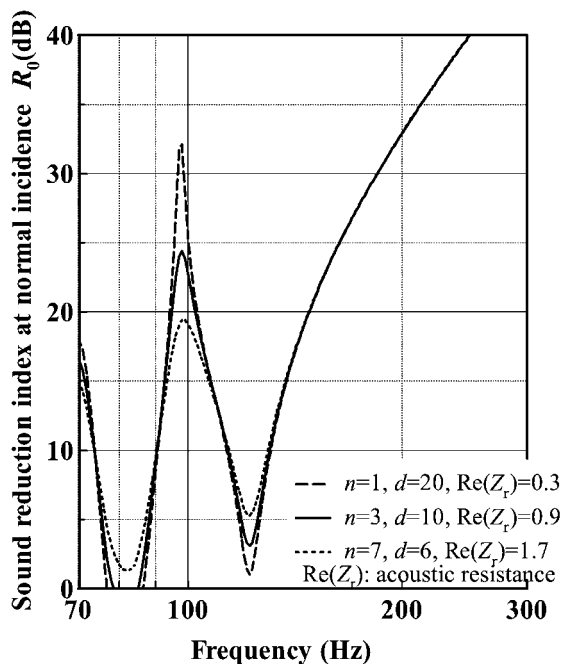


Fig. 8 Variation of predicted results of a wall with a resonator with number  $n$  and diameter  $d$  of holes when  $f_0 = 98$  Hz.

acoustic resistance, although the sound insulation at dips decreases slightly, as depicted in Figs. 8 and 9. In general, when a fibrous absorber is installed in the cavity, sound insulation increases with increasing internal sound reduction of the absorber, that is, with increasing density or thickness of the absorber [1–4]. However, from these results, it can be deduced that the sound insulation depends on the acoustic resistance but not on the sound absorption coefficient, because the absorption coefficient becomes unity at resonance frequency  $f_0$  when the acoustic resistance is unity.

Therefore, the acoustic impedance of the resonator must be very small, i.e., the diameter of the resonator must

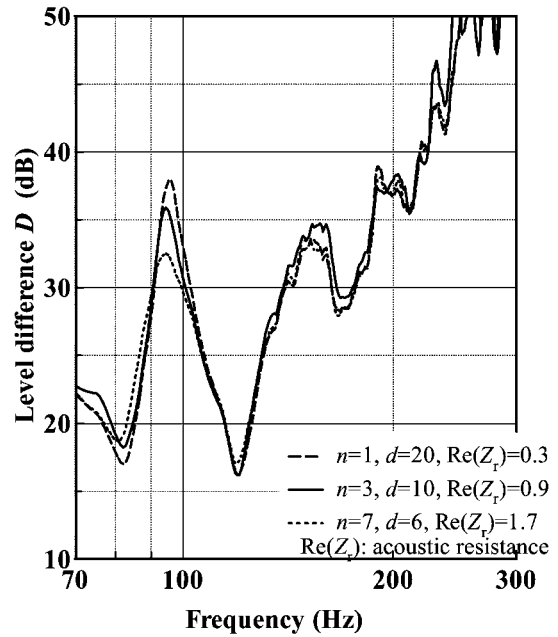


Fig. 9 Variation of measured results of a wall with resonator with number  $n$  and diameter  $d$  of holes when  $f_0 = 98$  Hz.

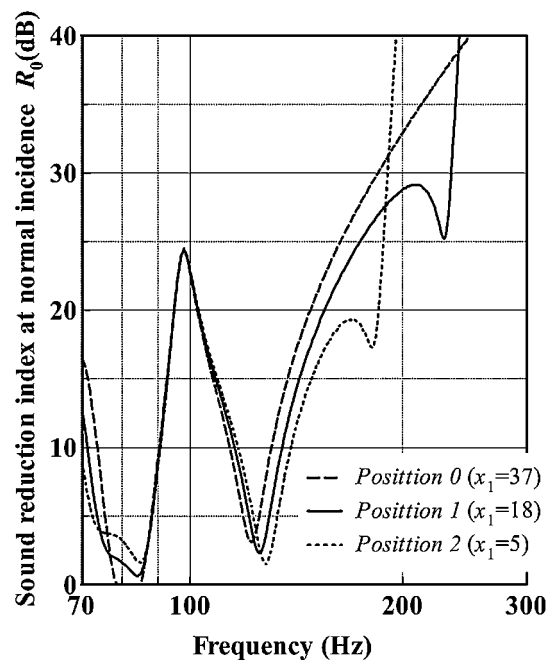


Fig. 10 Variation of predicted results of sound insulation with resonator position  $x_1$ ; see Fig. 1.

be very large, to obtain the maximum value of sound insulation at  $f_0$ .

#### 4.2. Influence of Position of Resonators in Cavity

Figure 10 shows predicted results of sound insulation for different positions of resonators in the cavity of the double-leaf partition. The resonators are the remotest from the board on the source side at “Position 0,” where  $(x_1, y_1)$

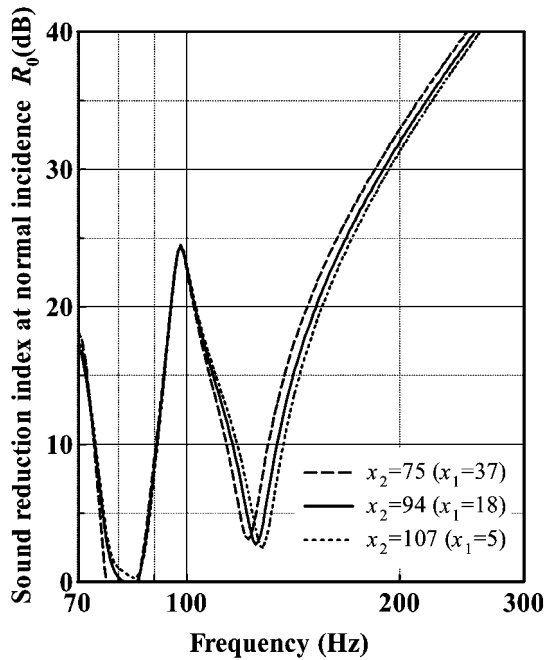


Fig. 11 Variation of predicted results of sound insulation with resonator thickness  $x_2$ ; see Fig. 1.

is (37 mm, 298 mm), as depicted in Fig. 3. At “Position 1,” they are placed almost at the cavity’s center, where  $(x_1, y_1)$  is (18 mm, 298 mm). Moreover, they are as close as possible to the board on the source side, at “Position 2,” where the position  $(x_1, y_1)$  is (5 mm, 298 mm). Those conditions, except the position, are shown in Table 1. The results are almost constant at the resonance frequency  $f_0$  whenever resonators are close to the board on the source side. However, in the cases of *Positions 1* and 2, new peaks and dips appear at higher frequencies than  $f_0$ . The peak and dip shift to the lower frequency side with decreasing distance  $x_1$ .

Figure 11 shows predicted results of sound insulation for different resonator thicknesses, although the resonator has no air cavity ( $x_3 = 0$ ) behind it. Only the resonator thickness  $x_2$  is increased, so that only the surface of resonators is close to the board on the source side. Here, the surface impedance on the resonator is constant among these cases. These results show that new peaks and dips do not appear merely upon the approach of the surface of the resonator to the board.

Figure 12 also shows measured results for different resonator positions (*Positions 0, 1, and 2*). The sound insulation changes when the resonator is distant from the board on the transmitting side. The new peaks and dips of sound insulation are not obvious. However, the sound insulation performance for *Position 2* is lower at frequencies around 160 Hz and higher at frequencies of 180–250 Hz than that for *Position 1*. This tendency in the measured results resembles that in the predicted results.

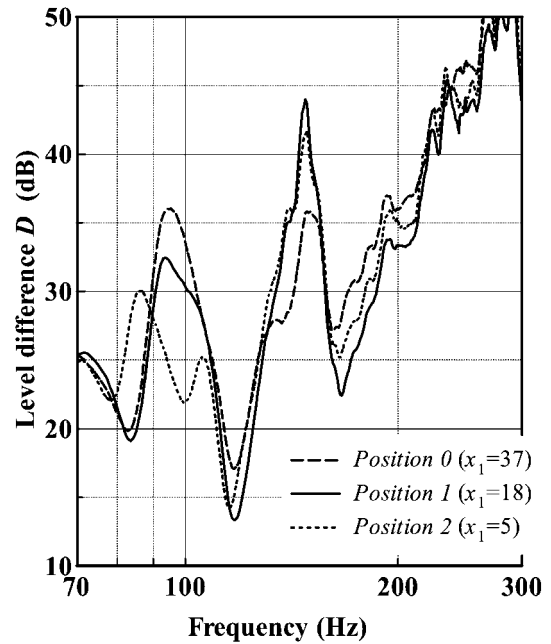


Fig. 12 Variation of measured results of sound level difference with resonator position  $x_1$ ; see Fig. 3.

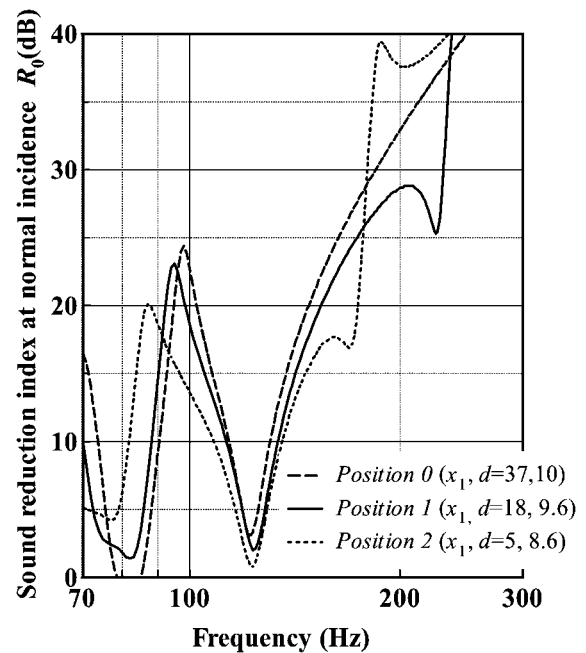


Fig. 13 Variation of predicted results of sound level difference with resonator position  $x_1$  and diameter  $d$ ; see Fig. 1.

However, the sound insulation at  $f_0$  decreases and the peak frequency is shifted to a lower frequency with decreasing distance  $x_1$ . Figure 13 shows an example of calculated sound insulation, assuming that the approach of resonators to the board decreases the diameter  $d$  of the hole to 9.6 mm (*Position 1*) and 8.6 mm (*Position 2*). The peak frequency ( $f_0$ ) is shifted to lower frequency and the value

decreases as the resonators approach the board. Therefore, this phenomenon can be considered to result from the change in the acoustic impedance in resonator holes because the board prevents the air mass in the holes from vibrating when the resonator approaches the board on the source side.

From these results, it can be deduced that the other peaks and dips in sound insulation occur at frequencies different from  $f_0$  because of the presence of the air cavity behind the resonator. The peak and dip frequencies depend on the air cavity thickness. In addition, the space in front of the resonator holes must remain large to prevent the sound insulation at  $f_0$  from decreasing.

#### 4.3. Improvement of Sound Insulation by Combined Use of Fibrous Absorber and Resonators

Mason and Fahy proposed that resonators having different frequencies were arranged in the cavity to expand the frequency range when sound insulation increased. However, the “two dips” always appeared by this case [7]. No other method to expand the frequency range has been proposed. Thus, to improve the sound insulation that had newly decreased at some frequencies after installing the resonator in the cavity, the air gap separating resonators in Layer III is filled with a fibrous absorber. The characteristic impedance  $Z_c$  and the propagation constant  $\gamma$  are obtained by substituting, into Eqs. (7a) and (7b),  $13,000 \text{ Pa s/m}^2$  as air-flow resistivity  $\sigma$ , which corresponds to glass wool with  $32 \text{ kg/m}^3$  density. Figure 14 shows predicted results of sound insulation for the case with the combined use of a 75-mm-thick fibrous absorber and resonators under the conditions presented in Table 1. The measured results are also presented in Fig. 15. Glass wool with a density of  $32 \text{ kg/m}^3$  and thickness of 75 mm was used as the fibrous absorber in these measurements.

Upon replacing air with fibrous absorber, the predicted results are improved and become almost equivalent to those of a double-leaf partition without resonators at the higher frequency where the dip occurs as a result of installing resonators. In contrast, the sound insulation at  $f_0$  is not dependent on whether the fibrous absorber is filled or not. In the measured results, installing glass wool also produces little change in the sound insulation at the 100 Hz band, which includes  $f_0$ ; it can improve the sound insulation at higher frequencies than the 125 Hz band in comparison with a double-leaf partition with resonators alone. Measured values drop at the 200 Hz and 250 Hz bands when nothing is installed in the cavity, because the standing wave with the calculated frequency of about 190 Hz, where the side of the specimen corresponds to  $1/2$  wavelength, occurred in the air cavity. Therefore, the measured results increase more than the predicted ones do in this frequency range, after installing the fibrous absorber.

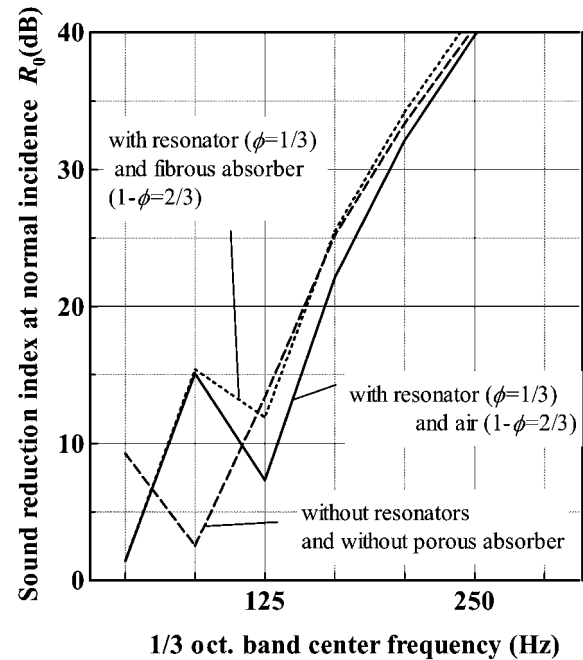


Fig. 14 Effect of fibrous absorber installed in air area of layer III on predicted results of sound insulation for wall with resonators.

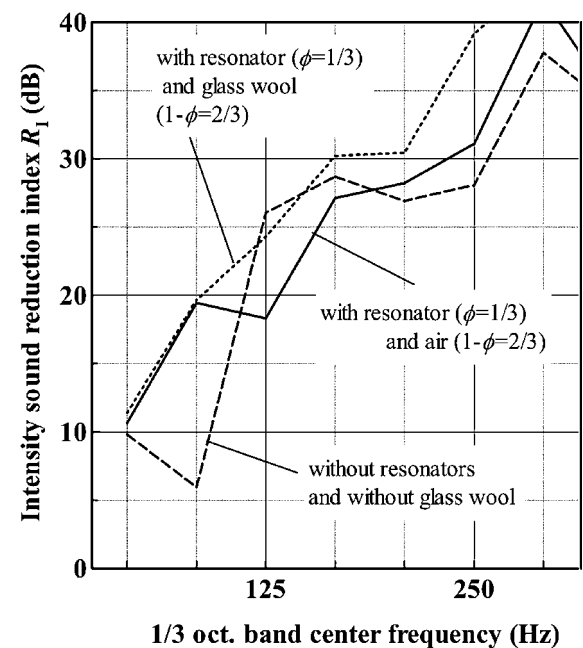


Fig. 15 Effect of glass wool installed in air area of layer III on measured results of sound insulation for wall with resonators.

These results demonstrate that sound insulation that had been decreased at higher frequencies than  $f_0$  by installing resonators, was further improved by the combined use of a fibrous absorber and resonators, while the peak value at  $f_0$  remained high. Therefore, the combined use is effective for increasing the sound insulation at frequencies higher than  $f_0$ .

## 5. CONCLUSIONS

We proposed a method of predicting the sound reduction index  $R_0$  at normal incidence for a double-leaf partition with Helmholtz resonators installed in the cavity. In this method, resonators were assumed to be independent of boards and studs and were assumed to be arranged uniformly and regularly. The sound reduction index  $R_0$  was calculated by the impedance transfer method. Experimental verification demonstrated that this prediction can qualitatively explain the effect of inserting the Helmholtz resonator into a cavity of a double-leaf partition on sound insulation, when the space in front of the resonator holes is sufficiently large. From results of this prediction and measurements, we found that installing a resonator in the cavity allows us to control the sound insulation at low frequencies.

- 1) The sound insulation at the mass-air-mass resonance frequency  $f_{\text{rmd}}$  is drastically increased by tuning the resonance frequency  $f_0$  of installed resonators to  $f_{\text{rmd}}$ , although two dips in sound insulation arise.
- 2) The sound insulation at  $f_0$  depends on the acoustic resistance of the resonators. It increases with decreasing acoustic resistance, although the sound insulation at the two dips is slightly changed.
- 3) The other peaks and dips of sound insulation occur at higher frequencies than  $f_0$  upon installing the air cavity behind the resonator. The frequency at which they appear depends on the thickness of the air cavity behind the resonator.
- 4) By combining resonators and fibrous absorber, the sound insulation at higher frequencies, where the dip occurs as a result of installing resonators, is improved. That at  $f_0$  retains its high performance. Consequently, the combination can improve sound insulation in the wide range of low frequencies including  $f_{\text{rmd}}$ .

## REFERENCES

- [1] R. A. Novak, "Sound insulation of lightweight double walls," *Appl. Acoust.*, **37**, 281–303 (1992).
- [2] J. D. Quirt and A. C. C. Warnock, "Influence of sound-absorbing material, stud type and spacing, and screw spacing on sound transmission through a double-panel wall specimen," *Proc. Inter-noise 93*, pp. 971–974 (1993).
- [3] A. Uris, A. Llopis and J. Llinares, "Effect of the rockwool bulk density on the airborne sound insulation of lightweight double walls," *Appl. Acoust.*, **58**, 327–331 (1999).
- [4] S. Sugie, J. Yoshimura and T. Iwase, "Sound insulation performance of double leaf partition improved with various types of absorbing materials at low frequencies," *Proc. Inter-noise 2006* (2006).
- [5] P. P. Narang, "Transforming wall studs to slit resonator studs for improving sound insulation in walls," *Appl. Acoust.*, **43**, 81–90 (1994).
- [6] R. A. Prydz, L. S. Wirt, H. L. Kuntz and L. D. Pope, "Transmission loss of a multilayer panel with internal tuned Helmholtz resonators," *J. Acoust. Soc. Am.*, **87**, 1597–1602 (1990).
- [7] J. M. Mason and F. J. Fahy, "The use of acoustically tuned resonators to improve the sound transmission loss of double-panel partitions," *J. Sound Vib.*, **124**, 367–379 (1988).
- [8] L. L. Beranek and G. A. Work, "Sound transmission through multiple structures containing flexible blankets," *J. Acoust. Soc. Am.*, **21**, 419–428 (1949).
- [9] K. Ookura and Y. Saito, "Transmission loss of multiple panels containing sound absorbing materials in a random incidence field," *Proc. Inter-noise 78*, pp. 637–642 (1978).
- [10] Y. Miki, "Acoustic properties of porous materials — Modification of Delany-Bazley models —," *J. Acoust. Soc. Jpn. (E)*, **11**, 19–24 (1990).
- [11] R. H. Bolt, "On the design of perforated facings for acoustic materials," *J. Acoust. Soc. Am.*, **19**, 917–921 (1947).
- [12] ISO 15186-1: 2000, "Acoustics — Measurement of sound insulation in buildings and of building elements using sound intensity — Part 1: Laboratory measurements" (2000).
- [13] ISO 140-3: 1995, "Acoustics — Measurement of sound insulation in buildings and of building elements — Part 3: Laboratory measurements of airborne sound insulation of building elements" (1995).
- [14] T. Iwase, M. Minowa, T. Maruyama and K. Yoshihisa, "Test method for sound insulation characteristics of light-weight double leaf wall by using small sample," *Proc. Inter-noise 2004* (2004).
- [15] C. Brutel-Vuilmet, C. Guigou-Carter, M. Villot and P. Jean, "Measurement of the sound reduction index as a function of the incidence angle by two different methods," *Build. Acoust.*, **13**, 33–48 (2006).

**Satoshi Sugie** was born in 1969. He received his B. Sc. and M. Sc. degrees from Gakushuin University in 1993 and 1995 respectively, and Dr. Eng. degree from Niigata University in 2009. His research interests are acoustic properties of acoustic material for sound absorption and insulation.

**Junichi Yoshimura** was born in 1950. He received his B. Eng., M. Eng. and Dr. Eng. degrees from Nihon University. His research interests are acoustic properties of building materials for sound absorption and insulation, and their measurement technique.

**Teruo Iwase** was born in 1948. He received his B. Eng., M. Eng. and Dr. degrees from the University of Tokyo. He was given the Sato Prize Paper Award from A. S. J. in 2000. He is Professor of Department of Architecture, Niigata University. His research interests are acoustic properties of sound material, such as absorption and insulation, recently more wide as porous asphalt, audible simulation and acoustical diagnosis.